

# STRUCTURAL AND DIELECTRIC STUDIES ON $\text{Sr}_{0.5-3y/2}\text{La}_y\text{Ba}_{0.5}\text{Nb}_2\text{O}_6$ CERAMIC SYSTEMS WITH VARIED SINTERING TIME AND La CONCENTRATION

S. R. ZAHARIMAN, <sup>#</sup>T. S. VELAYUTHAM \*, W. H. ABD MAJID, MARDHIAH SAID, W. C. GAN

Low Dimensional Materials Research Centre, Physics Department,  
University of Malaya, 50603 Kuala Lumpur, Malaysia

<sup>#</sup>E-mail: t\_selvi@um.edu.my

Submitted August 2, 2013; accepted November 25, 2013

**Keywords:** Dielectric properties, Curie temperature, Microstructure, Density

*Sr<sub>0.5</sub>Ba<sub>0.5</sub>Nb<sub>2</sub>O<sub>6</sub> (SBN50) ceramic doped with different concentration of Lanthanum, La according to stoichiometric formulation of Sr<sub>0.5-3y/2</sub>La<sub>y</sub>Ba<sub>0.5</sub>Nb<sub>2</sub>O<sub>6</sub> (LSBN) with y = 0.01, 0.03, 0.05 and 0.07 prepared using traditional ceramic method at the calcination temperature of 1200°C and sintered at 1300°C at varied sintering time. The effects of the sintering time and La<sup>3+</sup> substitution on the morphological, compositional, structural and electrical properties of the LSBN is presented using scanning electronic microscopy (SEM), energy dispersive spectroscopy (EDS), X-ray diffraction (XRD) and dielectric analysis. The XRD spectra confirm the presence of TTB structure in the ceramics. The Curie temperature (T<sub>c</sub>) of the ceramic identified from the dielectric studies performed in the temperature range of 28°C to 300°C. The temperature dependent dielectric exhibits broad peaks indicating a diffuse phase transition and relaxor behavior of the ceramic. The measured density of the samples is proportional to the sintering time and inversely proportional to the amount of the La<sup>3+</sup> substitution. The solubility limit of La<sup>3+</sup> ions in the SBN solid solution is at y ~ 0.05. This observation is also supported by the dielectric results where the dielectric properties of the ceramic deteriorate for y > 0.05 La substitution.*

## INTRODUCTION

Strontium barium niobate,  $\text{Sr}_x\text{Ba}_{1-x}\text{Nb}_2\text{O}_6$  (SBN) is one of the lead-free ferroelectric oxides which have attracted an increasing attention due to its large piezoelectric properties, high electro-optic coefficients and dielectric constant [1]. SBN is a typical relaxor system [2, 3] belonging to the tetragonal tungsten bronze (TTB) ferroelectric oxide family,  $\text{AB}_2\text{O}_6$ . The compositional and structural properties of this ceramic can be modified by adding a small amount of rare earth element (RE). Modifying the ceramic sometimes favors a higher reactivity of the grain and the densification rate while in some cases increase the grain size [4-7].

Literatures reported that doping of certain RE materials into SBN improved the pyroelectric and dielectric properties at room temperature [8]. Moreover, Curie temperature,  $T_c$  of the SBN doped with RE decreased tremendously from above 300°C to room temperature [9]. Although the effects of doping on the dielectric properties of SBN have been widely investigated [10] but an agreement on the effect of doping La on the  $T_c$  of SBN is not reached. The disorder crystal of SBN which has the random occupation of  $A_1$  and  $A_2$  sites influenced the ferroelectric properties and phase transition. Only

$\text{Sr}^{2+}$  cations occupy  $A_1$  sites while the  $A_2$  sites occupied by  $\text{Sr}^{2+}$  and  $\text{Ba}^{2+}$  cations. The ratio of Sr/Ba concentration at the  $A_2$  site is very important and when  $\text{La}^{3+}$  cations is doped to a system of constant Sr/Ba ratio, its properties will highly influenced by the dopant [10, 11]. The SBN properties are greatly affected by the type, amount of substitution, preparation methods and the condition of sintering [12]. In solid state reaction, the calcinations of powders were performed purposely to obtain a single phase and then preceded to sintering for densification [12]. Sintering has three predominant stages that are initial, intermediate, and final stages. However, only the final stages are investigated which mainly focused on the densification and the size of crystal grain where maximum values are desired [8].

The present work is dedicated to the study of the effects of varied sintering time and the addition of La substitute the Sr sites of the SBN ceramic in the compositional range of  $0 < y < 0.07$ . The structure and microstructure parameters such as density, volume, composition and grain size of the doped ceramic and electrical properties are presented here. The values of the dielectric constant were improved with respect to those reported previously while  $T_c$  shifted towards lower temperature.

## EXPERIMENTAL

The SBN and LSBN ceramics samples were obtained using conventional solid-state reaction method. The compounds were prepared by mixing high purity of  $\text{SrCO}_3$ ,  $\text{BaCO}_3$ ,  $\text{Nb}_2\text{O}_5$  and  $\text{La}_2\text{O}_3$  in stoichiometric quantities in agate mortar for 20 minutes. The mixed powders were calcined at  $1200^\circ\text{C}$  with ramp rate of  $5^\circ\text{C}$  for 5 hours to obtain single phase structure. The resulting powders were uniaxially die pressed at  $(400 \pm 20)$  bar of pressure into disks with a diameter of  $(13.00 \pm 0.01)$  mm and thickness of  $(1.50 \pm 0.01)$  mm. Then, the samples were sintered at 6 h, 12 h, and 24 h at  $1300^\circ\text{C}$ . In order to study the influence of La concentration towards the properties of SBN, an appropriate amount of mixtures according to stoichiometric formula  $\text{Sr}_{0.5-3y/2}\text{La}_y\text{Ba}_{0.5}\text{Nb}_2\text{O}_6$  with  $y = 0, 0.01, 0.03, 0.05$  and  $0.07$  were prepared and denoted as SBN50 or LSBN0, LSBN1, LSBN3, LSBN5 and LSBN7 respectively. The samples were sintered at  $1300^\circ\text{C}$  for 6 hours. As for electrical measurement, aluminium electrode was thermally evaporated on both sides of the samples. XRD measurements were performed to identify the crystallite size,  $D$  using Scherer's equation as shown in Equation 1.

$$D = \frac{k\lambda}{\beta \cos \theta} \quad (1)$$

where  $k = 0.9$ ,  $\lambda = 1.541 \text{ \AA}$ ,  $\theta$  is the diffraction peak angle and  $\beta$  is the full width at half maximum of the corresponding diffraction peak.

Density of the samples was obtained by measuring their volume and weight after sintering process. Morphology and the grain size of the samples were investigated by Field Emission Scanning Electron Microscope (FESEM). The dielectric permittivity of the samples was investigated using HP 4294A Impedance Gain Analyzer. The temperature of the samples was varied from  $30^\circ\text{C}$  to  $300^\circ\text{C}$  using hot chuck which was controlled by STC200 temperature controller.

## RESULTS AND DISCUSSIONS

The X-ray diffraction patterns of SBN50 ceramic before and after sintering with various sintering time 6 h, 12 h, and 24 h are shown in Figure 1. Basically, from Figure 1, it is observed that there is no shift in the reflection angles as the sintering time is increased which indicates that single phase (belonging to the SBN phase) is obtained for all the sintering time. The peaks became sharper and the full width at half maximum (FWHM) decreased as the sintering is increased indicating better crystallinity for samples sintered at longer time. Moreover, the increased intensity of (311) peak (SBN phase) with the increased sintering time, indicating that formation of pure TTB structure of SBN dependence on the sintering time. Normally, the undesired  $\text{SrNb}_2\text{O}_6$  (SN) phase identified at  $2\theta = 29.1$  while  $\text{BaNb}_2\text{O}_6$  (BN) phases observed at two characteristic peaks;  $2\theta = 28.4^\circ$  and

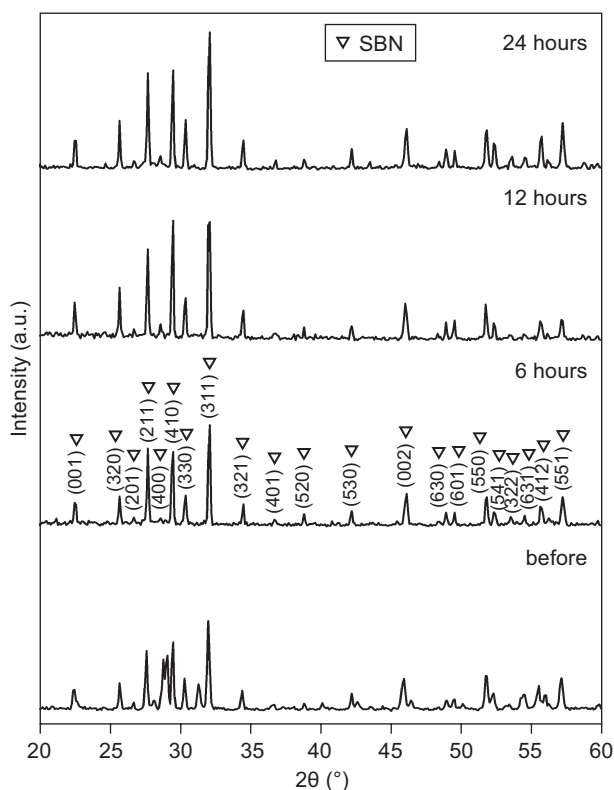


Figure 1. XRD patterns for SBN50 at different sintering time.

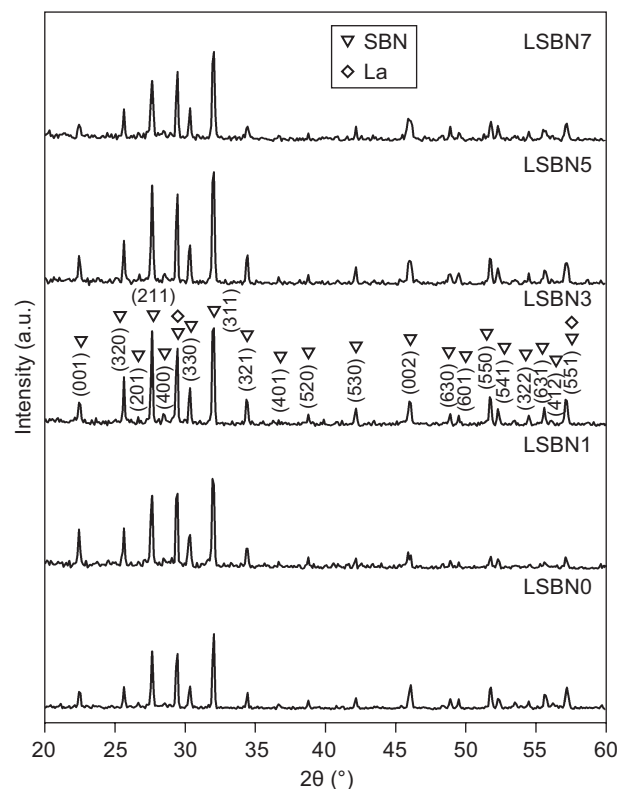


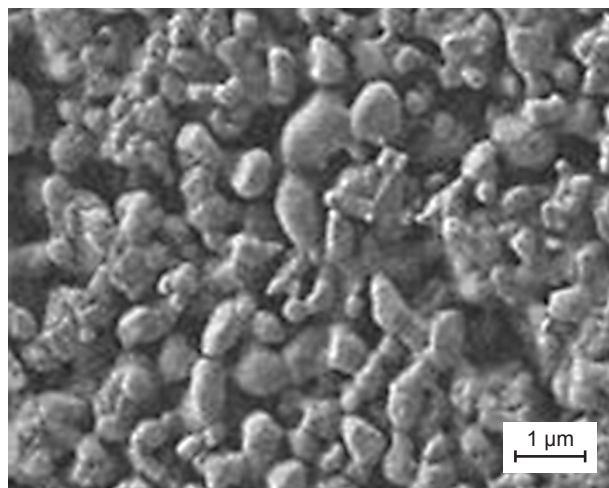
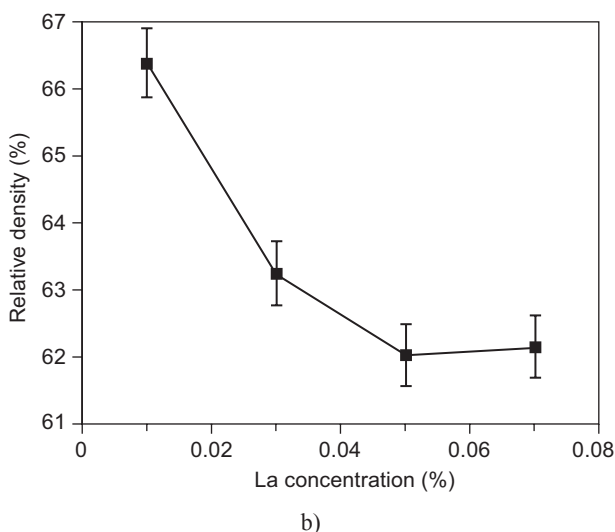
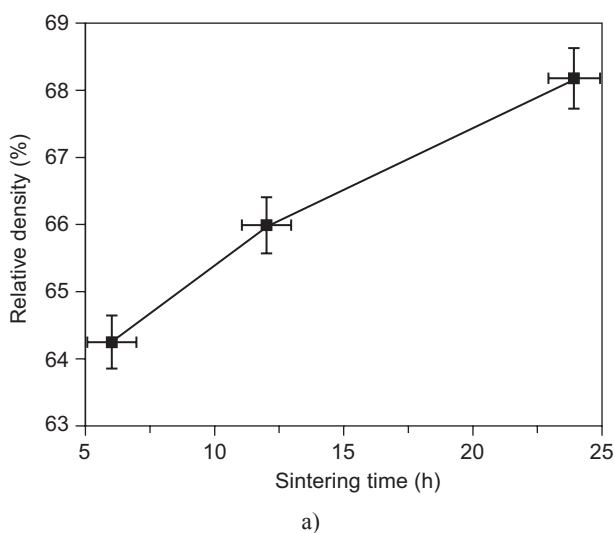
Figure 2. XRD patterns for SBN50 doped with different concentration of Lanthanum.

$2\theta = 29.8^\circ$ . Interestingly, in all sintering time, the undesired SN and BN phases had disappeared as it is combined to form TTB structure of SBN.

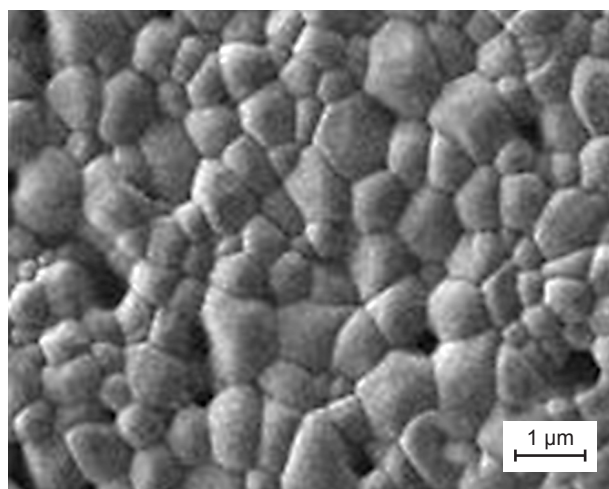
Figure 2 shows the XRD patterns of SBN50 (LSBN0), LSBN1, LSBN3, LSBN5 and LSBN7. It is observed that there is a small shifting of reflection angle as the concentration of La doped varied. Normally, La has a strong peak at  $2\theta = 27.59^\circ$  and  $57.2^\circ$ . From the spectra, it is observed that the presence of La phase coincide with the TTB structure of SBN at  $2\theta = 27.59^\circ$  and  $57.2^\circ$  peaks. In fact these peaks became sharper and the FWHM is decreased which indicates the enhancement in the crystallinity for samples doped with 1 - 5 % of La. However, the intensity (crystallinity) of the peaks decreased significantly at 7 % substitution of La.

Figure 3 shows the dependence of the relative density of SBN50 with the sintering time (a) and La concentration (b). It is noted that the density,  $\rho$  of the sample sintered at 6 h is increased from  $3.42 \text{ g/cm}^3$  to  $3.63 \text{ g/cm}^3$  at 24 h (see Figure 3a). The obtained results shows

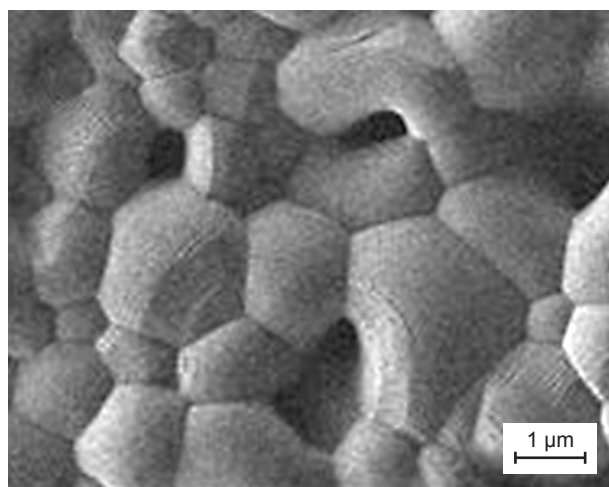
that the density is increased with the sintering time as predicted by the Coble's model [13]. The increase in density is due to the increase in the grain size of the samples during sintering process.



a) 6 h



b) 12 h



c) 24 h

Figure 3. The dependence of the relative density of SBN50 with (a) sintering time (b) La concentration.

Figure 4. FESEM micrographs of SBN50 sintered at  $1300^\circ\text{C}$  for a) 6 h, b) 12 h, c) 24 h.

Microstructure observation (see Figure 4) confirmed that the porosity of the grains decreased when the sintering time increased where the grains became closer. As a result, the movement of ions was restricted to each other. The average grain sizes measured for each samples are  $(1.17 \pm 0.06) \mu\text{m}$ ,  $(1.36 \pm 0.03) \mu\text{m}$  and  $(3.86 \pm 0.08) \mu\text{m}$  for 6 h, 12 h and 24 h respectively and these values are acceptable as it is in the range (1 - 3  $\mu\text{m}$ ) as reported in the literature [14]. The densification rates which are calculated over different time intervals from the gradient of the graph, decreased from 0.015 (from 6 h to 12 h) to 0.010 (12 h to 24 h). This indicates that the rate of densification of the material is inversely proportional to the sintering time. Coble assumed that the  $dp/dt$  is directly proportional to the diffusion coefficient,  $D$  [13]. Thus, it is reasonable to state that the diffusion process decreased with the increase of sintering time as observed from the results obtained here.

The relative density decreased when the concentration of La increased (1 - 5 %) (refer to Figure 3b). This is contrasting behavior with the previous observations

on PLZT [15] where the density increases with the concentration of La. The decrease of the density may be explained because the vacancies introduced by doping are bound to the impurity ions and unable to move freely through the crystal to expedite mass transfer. These bound vacancies reduce the concentration of the unbound vacancies and retard the diffusion [16]. The microstructure shown in Figure 5, shows that the grains of the samples increase with the increase of La concentration from 1 - 5 % then significantly decrease as 7 % of La is doped. The result is parallel to the decrease of the relative density as shown in Figure 3b.

Figure 6 and Table 1 shows the comparison of the EDX composition analysis for LSBN1 and LSBN3. 0.17 % atomic percentage of La in LSBN1 is observed compared to LSBN3 that is 0.43 %. The small difference of the atomic value of Sr and Ba indicates that the distribution of the mixture is saturated.

The frequency dependence of dielectric constant and loss for 6 h, 12 h and 24 h sintering time of SBN50 is shown in Figure 7. It is observed that both dielectric

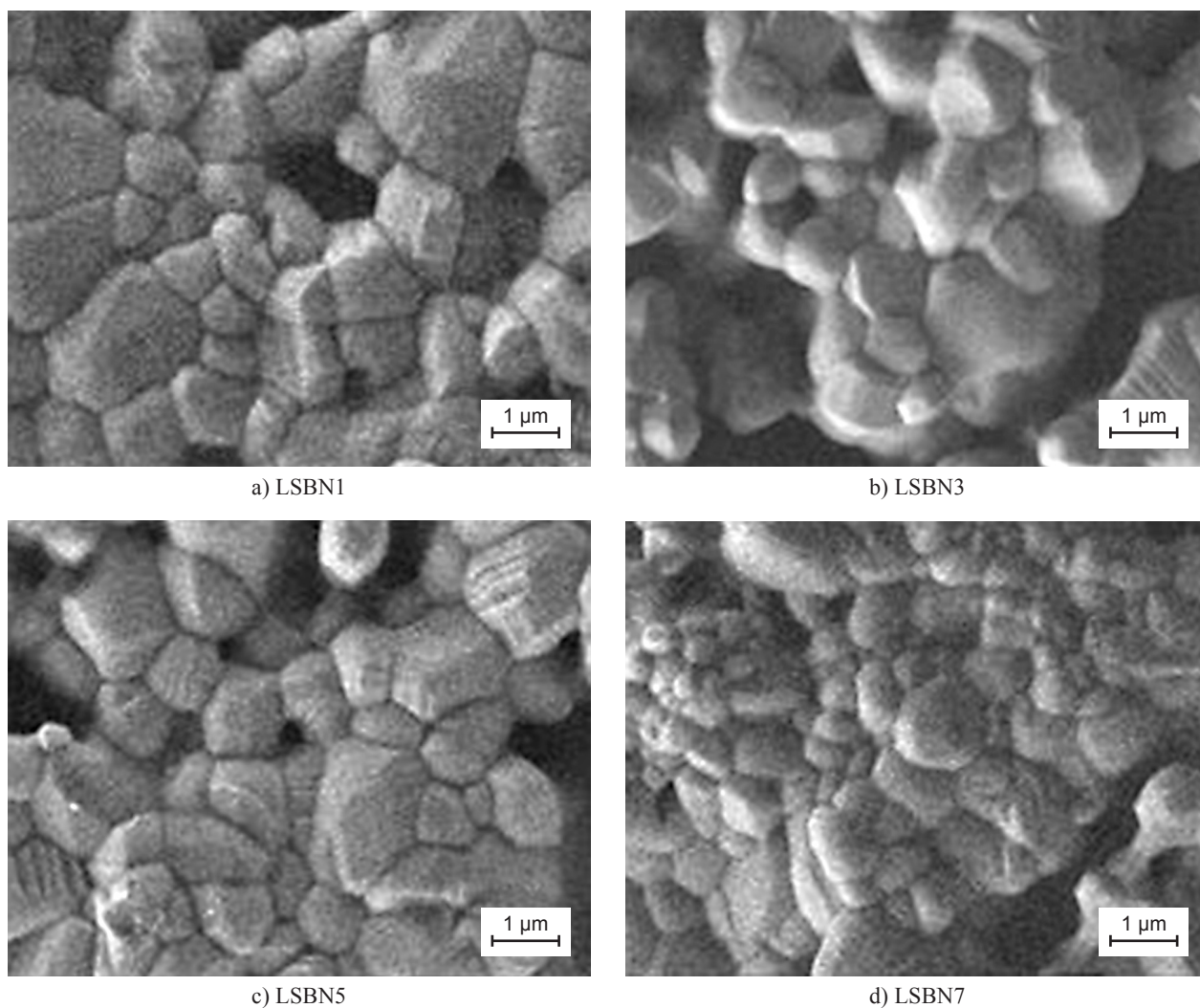


Figure 5. FESEM micrographs of LSBN ceramic; a) LSBN1, b) LSBN3, c) LSBN5, d) LSBN7.



constant and loss increase with the increase of the sintering time. For example at room temperature, the dielectric constant (at 100 Hz) increased from 78.03 for 6 h to 685.47 for 24 h. However, the increase of dielectric constant and loss with the sintering time is not desired for pyroelectric application because the figure of merit,  $F_v$  will be affected by both values as shown in Equation 2. The  $F_v$  can be calculated by :

$$F_v = \frac{\Gamma}{\sqrt{\varepsilon \tan \delta}} \quad (2)$$

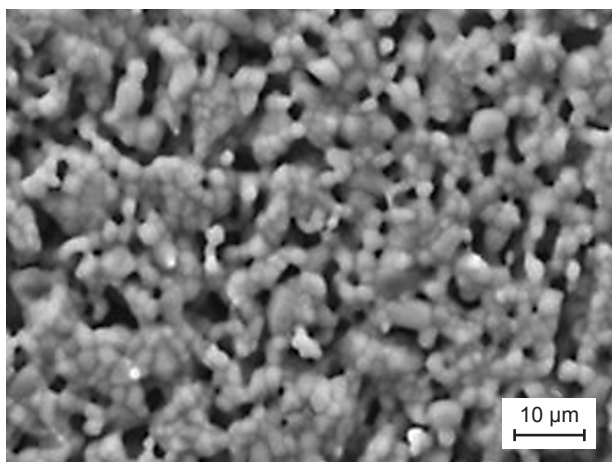
where  $\Gamma$ ,  $\varepsilon$  and  $\tan \delta$  represent the pyroelectric coefficient, dielectric constant, and dielectric loss respectively. Since  $F_v$  is inversely proportional to  $\varepsilon$  and  $\tan \delta$ , the sample sintered at 6 h is predicted to give highest  $F_v$  compared to the one sintered at 24 h.

The temperature dependence of dielectric constant and loss for SBN50 at different sintering times measured at 100 kHz is displayed in Figure 8. At 24 h sintering time, a maximum dielectric constant is observed at 149°C which is the Curie temperature,  $T_c$ . It is noted that  $T_c$  is not observed for 6 h and 12 h as they seem to be larger than 300°C. Besides, the value of the dielectric constant is greatly influenced by the temperature and the grain size.

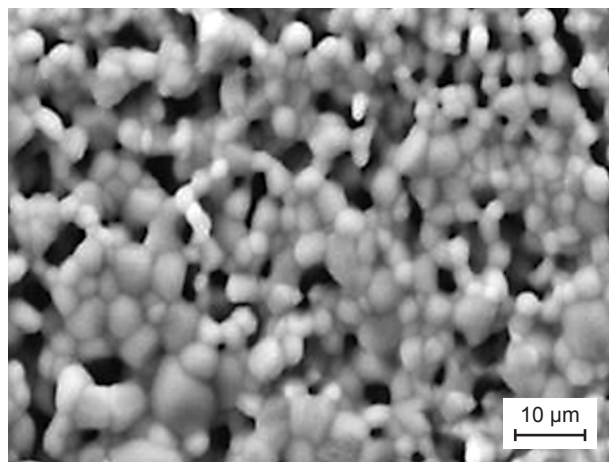
The frequency and temperature dependence of the dielectric constant for La doped SBN from are shown in Figure 9a and b respectively. As the concentration of the La increased the dielectric constant increased except for 7 % (see Figure 9a). In fact, at 7 % doped La, the dielectric constant significantly decreased to lower than 1 % La doped dielectric constant value. The observation matches well with the XRD pattern where the intensity of the spectra decreased indicating the crystallinity of the 7 % La doped ceramic decreased. The solubility limit of  $\text{La}^{3+}$  in the SBN solid solution seems to be at ~ 5 % La doped. The additions of La which exceed the solubility

Table 1. Weight and atomic percentages for LSBN1 and LSBN3 based on EDX composition analysis.

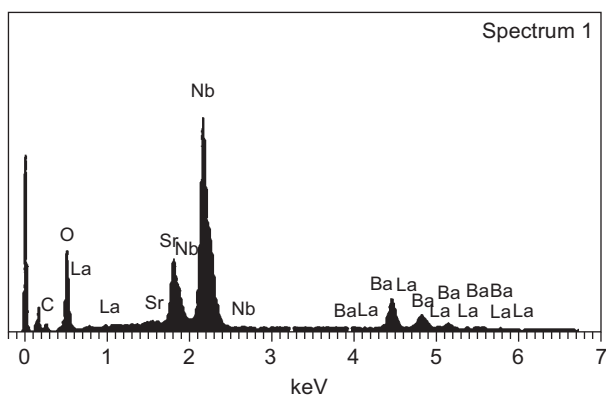
Element	LSBN1		LSBN3	
	Weight (%)	Atomic (%)	Weight (%)	Atomic (%)
C	7.17	19.45	5.82	17.28
O	29.28	59.63	26.29	58.62
Sr	9.26	3.44	8.29	3.37
Nb	40.49	14.20	42.30	16.24
Ba	13.07	3.10	15.63	4.06
La	0.74	0.17	1.67	0.43



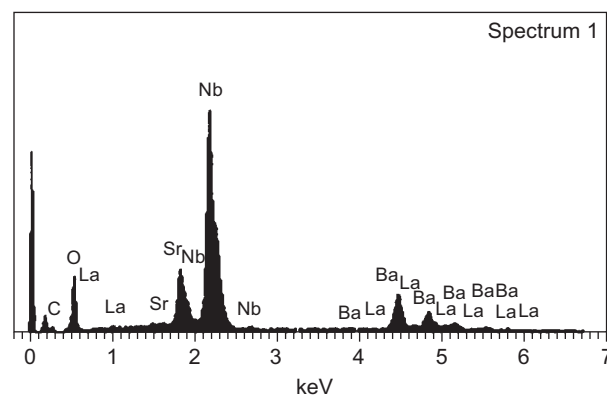
a)



b)



c)



d)

Figure 6. FESEM micrographs of LSBN ceramic (a) LSBN1, (b) LSBN3, (c) LSBN5, (d) LSBN7.

limit deteriorate the dielectric and structural properties of the sample [11]. As for temperature dependence dielectric constant spectra (Figure 9b), a broad transition from RT to 300°C is observed in all cases except LSBN0 and LSBN7. This is a typical behavior for ferroelectric materials with diffuse phase transition. The existence of polar micro regions above the nominal transition temperature provokes the diffuse phase transition mainly because of composition and local polarization [17]. Besides,  $T_c$  for 1 % and 3 % doped La concentrations are identified as 169°C and 50°C respectively. These values are lower than those reported earlier by other groups [10, 18] which is consider a very good improvement since the  $T_c$  is near to RT. As the La concentration is increased

to 5 %, it is observed that the  $T_c$  is lower than the room temperature since the spectra seems to increase at lower temperature below the measured range. However, as for 7 % of La there isn't any trend that can be identified as  $T_c$ .

## CONCLUSION

The dielectric properties of SBN are influenced by the sintering time and the ratio of Lanthanum doped. As the sintering time is longer, the dielectric constant and loss increase while the Curie temperature of SBN50 decrease. At 24 h sintering time, its Curie temperature decreases to 149°C. At 6 h of sintering time, the SBN

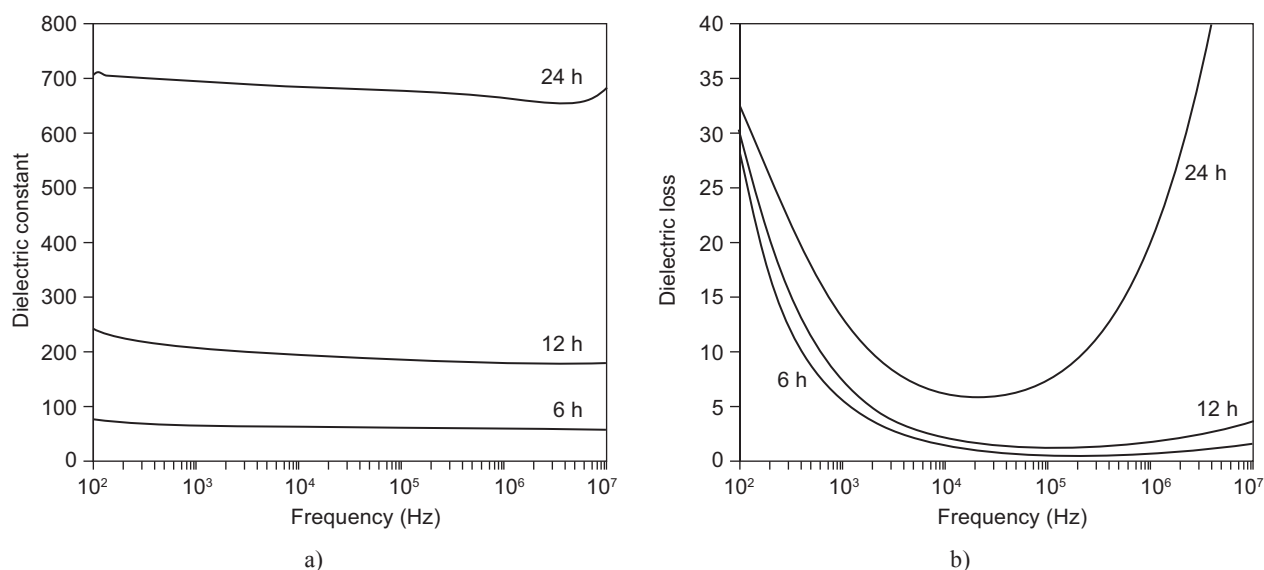


Figure 7. The frequency dependence of dielectric constant (a) and dielectric loss (b) measured at room temperature for various sintering time of SBN50.

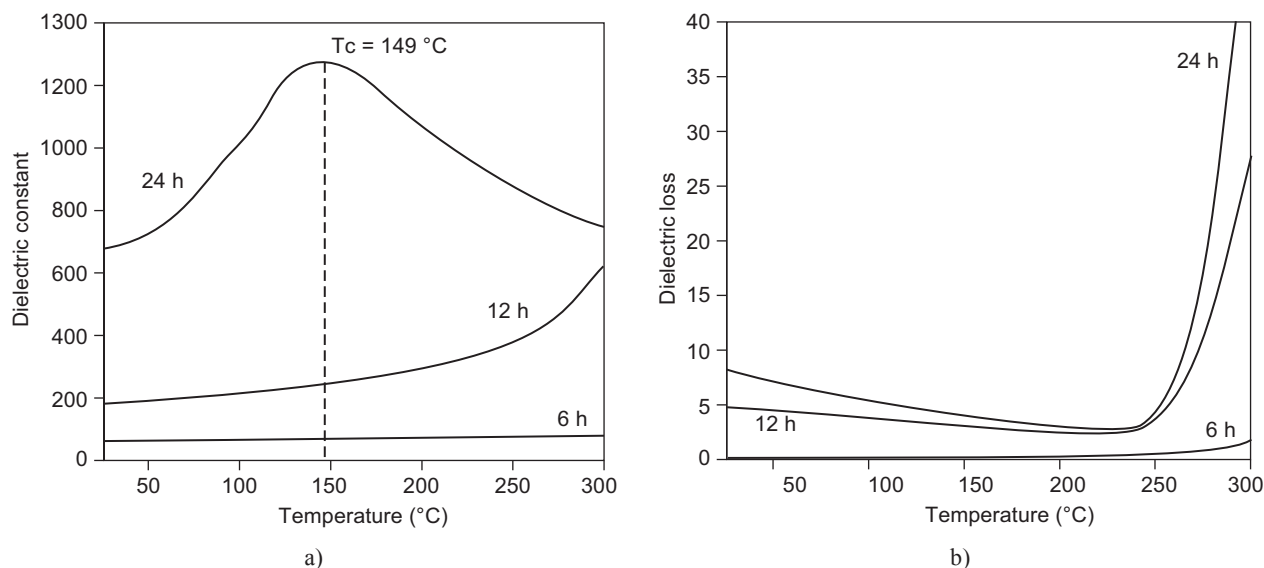


Figure 8. Temperature dependence spectra of dielectric constant (a) and dielectric loss (b) measured at 100 kHz of varied sintering time for SBN50.

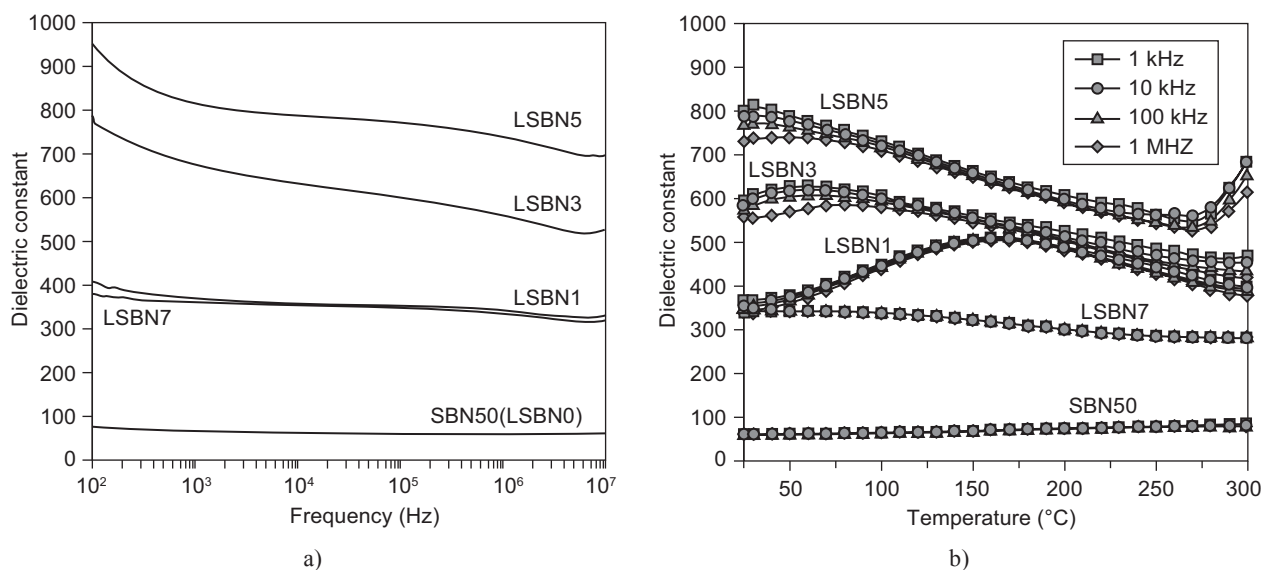


Figure 9. The frequency dependence of (a) dielectric constant measured at room temperature and (b) temperature dependence of dielectric constant at various frequency and concentration of La.

shows a single phase XRD pattern and SN and BN phases disappear to combine and form TTB structure of SBN. In addition, at 6h sintering time, the ceramic exhibits the lowest dielectric constant and loss which therefore, can be a best pyroelectric detector since the  $F_v$  of the ceramic will be higher. The crystallinity of the sample increases with the sintering time and the concentration of Lanthanum doped. The density of SBN50 increase as the sintering time is longer due to the increase of the grain size but the densification is inversely proportional to the sintering time. It is observed that the density of SBN50 is decreased as the ratio of Lanthanum doped is increased. As the concentration of Lanthanum doped is increased, the dielectric constant and loss increase while the Curie temperature,  $T_c$  decrease tremendously nearing to room temperature. It is noted that at 7 % of La doped, the crystallinity, grain size, dielectric constant and loss are degraded. This shows the existence of the solubility limit of the Lanthanum ions in the SBN solid solution.

#### Acknowledgement

*This work is supported by University of Malaya through grant number: RG258-13AFR & RP007A-13AFR*

#### REFERENCES

1. Hao X., Yang Y. F.: *J. Mater. Sci.* **42**, 3276 (2007).
2. Liu S. T., Bhalla A. S.: *Ferroelectrics* **51**, 47 (1983).

3. Smolenskii G. A., Isupov V. A., Ktitorov S. A., Trepakov V. A., Yushin N. K.: *Russ. Phys. J.* **22**, 1 (1979).
4. Luna-Lopez J. A., Portelles J., Raymond O., Siqueiros J. M.: *Mater. Chem. Phys.* **118**, 341 (2009).
5. Malyskina O. V., Movchikova A. A., Pedko B. B., Boitsova K. N., Kiselev D. A., Kholkin A. L.: *Ferroelectrics* **373**, 114 (2008).
6. Lehnen P., Dec J., Kleemann W., Woike T., Pankrath R.: *Ferroelectrics* **268**, 113 (2002).
7. Caldiño U., Molina P., Ramirez M. O., Jaque D., Bausa L. E., Zaldo C., Ivleva L., Bettinelli M., Solé J. G.: *Ferroelectrics* **363**, 150 (2008).
8. Maciolek R. B., Liu S. T.: *J. Electron. Mater.* **4**, 517 (1975).
9. Liu S. T., Maciolek R. B.: *J. Electron. Mater.* **4**, 91 (1975).
10. Guerrero F., Portelles J. J., González I., Fundora A., Amorin H., Siqueiros J. M., Machorro R.: *Solid State Commun.* **101**, 463 (1997).
11. Amorin H., Portelles J., Guerrero F., Fundora A., Martínez E., Siqueiros J. M.: *J. Mater. Sci.* **35**, 4607 (2000).
12. Kumar S. N., Kumar P., Agrawal D. K.: *Ceram. Int.* **38**, 5243 (2012).
13. Coble R. L.: *J. Appl. Phys.* **32**, 787 (1961).
14. Zhang J., Wang G., Gao F., Mao C., Cao F., Dong X.: *Ceram. Int.* **39**, 1971 (2013).
15. El-Salam F. A., Tawfik A., Eatah A. I.: *Ferroelectrics* **65**, 131 (1985).
16. Guerrero F., Portelles J. J., Amorin H., Fundora A., Siqueiros J., Hirata G.: *J. Eur. Ceram. Soc.* **18**, 745 (1998).
17. Cross L. E.: *Ferroelectrics* **76**, 241 (1987).
18. Guerrero F., Amorin H., Portelles J., Fundora A., Siqueiros J. s., Hirata G., Aguilera S.: *Journal of Electroceramics* **3**, 377 (1999).